



## RAPID COMMUNICATION

# Pivotal role of cytosolic phospholipase PLA2G4A in the pathogenesis of *FLT3*-ITD-mutated acute myeloid leukemia

Internal tandem duplication of FMS-like tyrosine kinase 3 (*FLT3*-ITD) is one of the most common genetic alterations in human acute myeloid leukemia (AML) and confers a poor prognosis for the disease.<sup>1</sup> Though several *FLT3* inhibitors have been approved in AML, their clinical benefits are still unsatisfactory due to primary refractory and drug resistance. Therefore, it may be crucial to develop novel therapeutics for *FLT3*-ITD<sup>+</sup> AML.

We previously demonstrated that Follistatin is a novel biomarker and therapeutic target in *FLT3*-ITD<sup>+</sup> AML.<sup>2</sup> This prompted us to identify more therapeutic targets in *FLT3*-mutated AML. To this end, here we first identified the differentially expressed genes (DEGs,  $n = 928$ ,  $|FC| > 1.5$ ,  $P < 0.001$ , LinkedOmics database) in *FLT3*-mutated (*FLT3*<sup>mut</sup>) AML comparing to those of *FLT3*-wildtype (*FLT3*<sup>wt</sup>). Among these DEGs, *PLA2G4A*, *IL2RA*, *C10orf128*, *TREML2*, *SCHI P1*, *PRDM16*, *IL10*, *CCDC113*, *MAN1C1*, *MLF1*, and *RBM11* were highlighted based on their significant prognostic values in human AML (Fig. S1, GEPIA database,  $P < 0.005$ , overall survival). Interestingly, *PLA2G4A* and *IL2RA* were FDA-approved drug targets (Fig. 1A), which may be further explored for drug repurposing in *FLT3*-mutated AML in pre-clinical models. Recently, *IL2RA* has been reported to be positively correlated with *FLT3*-ITD mutations and disease aggressiveness of AML, confirming the validity of our screening algorithm. *PLA2G4A* encodes for the cytosolic phospholipase A2 $\alpha$  (cPLA2 $\alpha$ ), which is the rate-limiting enzyme in phospholipid metabolism and plays an important role during tumorigenesis.<sup>3</sup> However, the pathogenic role of *PLA2G4A* in *FLT3*-mutated AML is still elusive.

*PLA2G4A* is highly expressed in AML cell lines (Fig. S2A, CCLE database) and TCGA-LAML cases comparing to normal blood cells (Fig. 1B, GEPIA program). High expression of *PLA2G4A* is associated with dismal prognosis (Fig. 1C,

Oncolnc program), FAB-M5 subtype (Fig. 1D, UALCAN program), high risk karyotypes [MLL-rearranged (MLL-r) and complex, Fig. S2B, BloodSpot program], age of patients (Fig. S2C), and *FLT3* mutations in public TCGA-LAML database (Fig. 1E–i) or Leukemia MILE study (Fig. 1E–ii). The upregulation of *PLA2G4A* in *FLT3*-mutated AML was validated using our archived primary AML samples (Fig. 1E–iii). These data showed that *PLA2G4A* was a poor prognostic marker and highly expressed in *FLT3*-mutated AML.

Consistent with our previous observations,<sup>4</sup> overexpression of *FLT3*-ITD resulted in expansion of *mpo* + myeloid cells in zebrafish embryos (Fig. S3). *FLT3*-ITD-expressing embryos showed increased expression of *pla2g4aa* (human *PLA2G4A* orthologue) (Fig. 1F, red arrows). In addition, kidney marrow (equivalent to human bone marrow) from *FLT3*-ITD-transgenic zebrafish showed myeloproliferative neoplasm (MPN)-like phenotype and increased expression of *pla2g4aa* (Fig. 1G). *FLT3*-ITD mutations resulted in activation of ERK, AKT and STAT5 in AML (Fig. S4A, B). Importantly, treatment of *FLT3* inhibitor (Fig. 1H, quizartinib) or ERK inhibitor (Fig. 1I, ulixertinib), but not AKT or STAT5 inhibitors (Fig. S4C, D), reduced the expression and phosphorylation of *PLA2G4A* in *FLT3*-ITD<sup>+</sup> MOLM-13 AML cells. We and other groups demonstrated that p90RSK was important for *FLT3*-ITD/ERK signaling in AML.<sup>2</sup> Treatment of p90RSK inhibitor (BID-1870) effectively reduced the transcription of *PLA2G4A* in MOLM-13 cells (Fig. 1J). Moreover, quizartinib-resistant MOLM-13 cells showed significant upregulation of *PLA2G4A* (Fig. 1K), suggesting that *PLA2G4A* may play an important role during tyrosine kinase inhibitor (TKI) resistance. These data indicated that *FLT3*-ITD/ERK/p90RSK/*PLA2G4A* signaling may play an important role in the progression and drug resistance of AML.

This prompted us to test the effects of *PLA2G4A* inhibition in *FLT3*-ITD<sup>+</sup> MOLM-13 cells *in vitro* and *in vivo*. Genetically, knockdown of *PLA2G4A* significantly inhibited MOLM-13 cell growth *in vitro* (Fig. 1L), induced apoptosis

Peer review under responsibility of Chongqing Medical University.

<https://doi.org/10.1016/j.gendis.2022.02.002>

2352-3042/© 2022 The Authors. Publishing services by Elsevier B.V. on behalf of KeAi Communications Co., Ltd. This is an open access article under the CC BY-NC-ND license (<http://creativecommons.org/licenses/by-nc-nd/4.0/>).

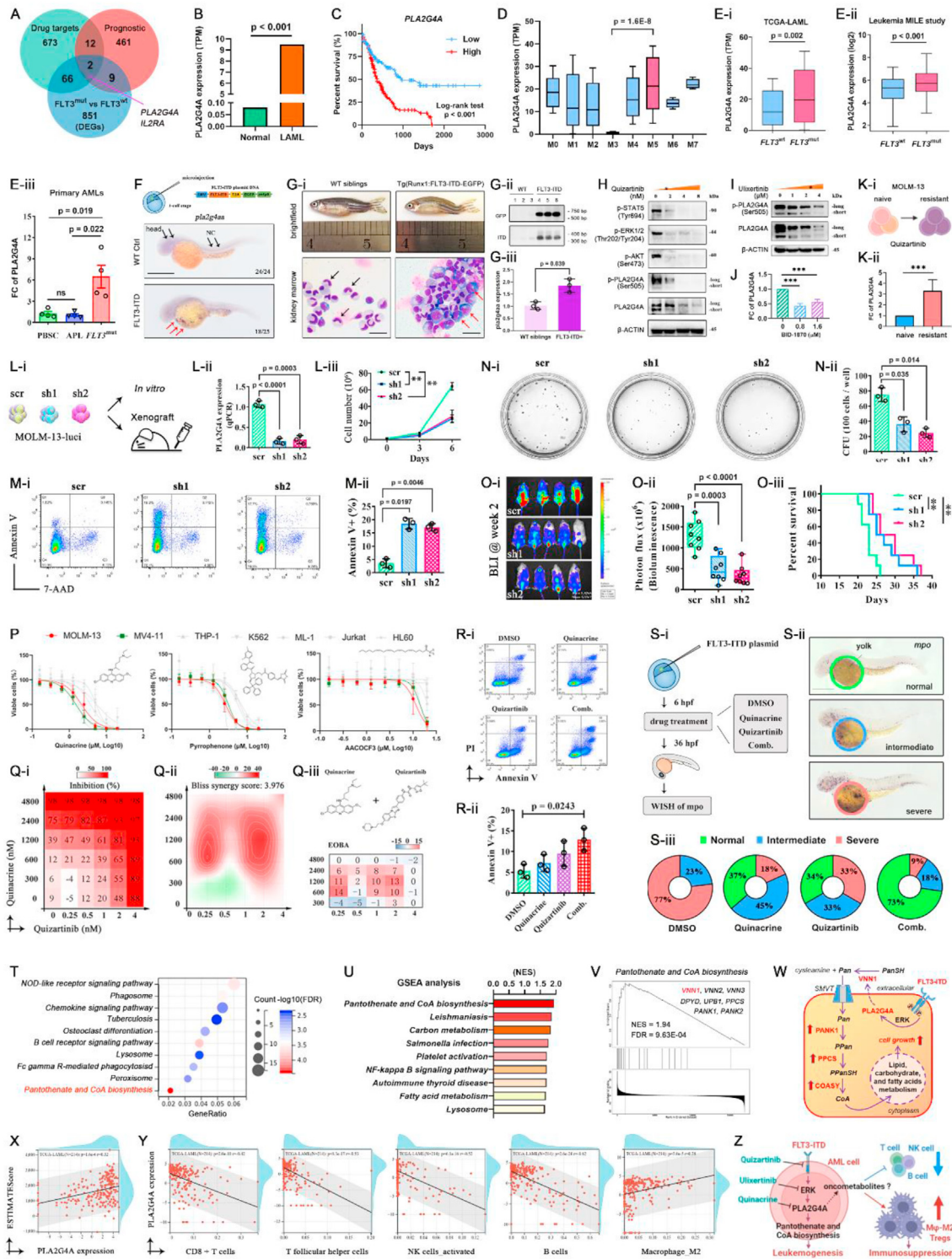


**Figure 1** Implications of PLA2G4A in FLT3-ITD<sup>+</sup> AML. (A) Venn diagram showing the overlapping of FDA-approved drug targets (green circle, HPA database), DEGs (*FLT3*<sup>mut</sup> vs. *FLT3*<sup>wt</sup>) in AML (blue circle, LinkedOmics database, |FC| > 1.5, *P* < 0.001) and prognostic markers in AML (red circle, GEPIA database, overall survival, *P* < 0.005, logrank test). (B) *PLA2G4A* expression in normal blood (GTEx database, *n* = 70) and AML cases (TCGA-LAML database, *n* = 173) was analyzed by GEPIA program. (C) Overall survival of TCGA-LAML patients was analyzed by Oncolnc program based on *PLA2G4A* expression (logrank test). (D, E) Expression profile of *PLA2G4A* in FAB subtypes (D, UALCAN database) and *FLT3*-mutated AML from TCGA-LAML (E-i, UALCAN program), leukemia MILE study (E-ii, Bloodspot program) and our primary AML samples (E-iii, RT-qPCR). (F) Whole mount *in situ* hybridization assay showing the expression of *pla2g4a* in wild-type control and *FLT3*-ITD plasmid-injected zebrafish embryos at 36 hpf, respectively. Scale bars = 500 μm. NC, notochord. (G) Morphology of blood cells (G-i, Wright-Giemsa staining), genotyping of *FLT3*-ITD transgene (G-ii) and expression of *pla2g4a* (G-iii, RT-qPCR) in kidney marrow samples from age-matched wild-type siblings and *FLT3*-ITD-transgenic

(Fig. 1M), reduced the clonogenicity of MOLM-13 cells *in vitro* (Fig. 1N), reduced leukemia burden and significantly prolonged the survival of MOLM-13-engrafted animals *in vivo* (Fig. 1O). Pharmaceutically, PLA2G4A inhibitors (quinacrine, pyrrophenone and AACOCF3) preferentially suppressed the growth of *FLT3*-ITD-mutated MOLM-13 and MV4-11 leukemia cell lines comparing to those of *FLT3*-WT (THP-1, K562, ML-1, Jurkat, and HL-60) (Fig. 1P). In addition, quinacrine effectively synergized with *FLT3* inhibitor quizartinib to suppress the growth of MOLM-13 cells *in vitro* (Fig. 1Q) by inducing apoptosis (Fig. 1R). Combined treatment of quizartinib and quinacrine also effectively ameliorate the myeloid expansion phenotype in *FLT3*-ITD-expressing zebrafish model *in vivo* (Fig. 1S). The synergism between quinacrine and other clinically available *FLT3* inhibitors (midostaurin, gilteritinib, sorafenib, and crenolanib) was also demonstrated in MOLM-13 cells *in vitro* (Fig. S5). These data indicated that PLA2G4A was important for the survival of *FLT3*-ITD<sup>+</sup> AML.

The above observations prompted us to explore the underlying mechanism(s) of PLA2G4A-mediated leukemogenesis. The RNA-sequencing (RNA-Seq) data showed that PLA2G4A was significantly associated with a list of genes (Fig. S6A, B) which were enriched in distinct pathways by KEGG analysis (Fig. 1T). Among these pathways, "Pantothenate and CoA biosynthesis" was most significant. The "Pantothenate and CoA biosynthesis" was also highlighted by GSEA analysis of PLA2G4A-correlated genes (Fig. 1U, V; Fig. S6C–J). Coenzyme A (CoA) functions as a carrier of acetyl and acyl groups in eukaryotes and plays a critical role in synthetic and degradative metabolic processes. In particular, the pantetheinase Vanin-1 (*VNN1*), from "Pantothenate and CoA biosynthesis" pathway, was significantly associated with PLA2G4A (Fig. S7A), poorer prognosis of AML (Fig. S7B), and *FLT3* mutations (Fig. S7C). In addition, pantothenate kinase 1 (*PANK1*) which catalyzes the first and rate-limiting enzymatic reaction in CoA

biosynthesis, was also significantly increased in *FLT3*-mutated AML (Fig. S7D). Moreover, phosphopantothoeylcysteine synthetase (*PPCS*) and Coenzyme A synthase (*COASY*) which are crucial for the last two steps of CoA biosynthesis, were significantly upregulated in *FLT3*-mutated AML (Fig. S7E, F). These observations indicated that *FLT3*-ITD/ERK/PLA2G4A/*VNN1*-mediated pantothenate and CoA biosynthesis may play an important role during the progression of AML (Fig. 1W).

It has been reported that colorectal cancer with high PLA2G4A expression can educate  $\gamma\delta$  T cells into CD39<sup>+</sup> $\gamma\delta$  Tregs to promote tumor progression and metastasis.<sup>5</sup> However, the immunological value of PLA2G4A in AML is still unclear. We showed that expression of PLA2G4A was significantly associated with immune infiltrations in human AML by ESTIMATE analysis using SangerBox program (Fig. 1X,  $P = 1.6E-6$ ,  $R = 0.32$ ). AML cases with high PLA2G4A expression was associated with the decrease of CD8<sup>+</sup> T cells, T follicular helper cells, activated NK cells, and B cells by CIBERSOR analysis (Fig. 1Y; Fig. S8A). Increase of M2 macrophage (Fig. 1Y) and Tregs (Fig. S8B–D) were significantly associated with high PLA2G4A expression in AML by CIBERSOR and QUANTISEQ analysis, respectively. These observations indicated that upregulation of PLA2G4A may perturb the tumor microenvironment in human AML.

Collectively, cytosolic phospholipase PLA2G4A is highly expressed in *FLT3*-ITD<sup>+</sup> AML and in *FLT3*-ITD-expressing zebrafish model. Transcriptionally, upregulation of PLA2G4A is mediated by *FLT3*-ITD/ERK/p90RSK signaling. Genetically, knockdown of PLA2G4A suppresses the growth of *FLT3*-ITD<sup>+</sup> AML cells *in vitro* and *in vivo*. Pharmacologically, inhibition of PLA2G4A synergizes with clinically available *FLT3* inhibitors *in vitro* and in *FLT3*-ITD-overexpressed zebrafish *in vivo* model. Mechanistically, upregulation of PLA2G4A is implicated in "pantothenate and CoA biosynthesis"-mediated leukemogenesis and associated with immunosuppressive microenvironment in human AML (Fig. 1Z).

zebrafish. (H, I) Expression and phosphorylation of PLA2G4A were tested by Western Blotting after treatment of *FLT3* inhibitor (H, quizartinib) and ERK inhibitor (I, ulixertinib) in MOLM-13 cells for two days. The asterisks indicated the IC<sub>50</sub> concentration of drugs. (J) Transcription of PLA2G4A after treatment of p90RSK inhibitor BID-1870 in MOLM-13 cells *in vitro*. (K) PLA2G4A was upregulated in quizartinib-resistant MOLM-13 cells *in vitro*. (L–O) Knockdown of PLA2G4A reduced the growth of MOLM-13 cells *in vitro* (L), induced apoptosis (M), reduced colony-forming units (N), reduced the engraftment of MOLM-13 cells and prolonged the survival of MOLM-13-engrafted mice (O). (P, Q) The anti-leukemic effects of PLA2G4A inhibitors quinacrine, pyrrophenone, or AACOCF3 were tested in MOLM-13, MV4-11, THP-1, K562, ML-1, Jurkat, and HL-60 cells *in vitro* (P). Synergism between quinacrine and quizartinib was tested in MOLM-13 cells *in vitro* (Q-i). Bliss synergy score (Q-ii, SynergyFinder), and EOBA score (Q-iii) were calculated to predict the potential synergism of two drugs. (R) Detection of apoptosis after combined treatment of quizartinib and quinacrine in MOLM-13 cells *in vitro*. (S) Overexpression of *FLT3*-ITD resulted in expansion of *mpo* + myeloid cells in zebrafish embryos (S-i and S-ii). The myeloid phenotypes were classified into three groups: normal, intermediate, and severe. Intermediate level indicated that there was increased expression of *mpo* in the yolk sac but no clustering was observed (blue circle). Severe level was defined as significant ectopic expression of *mpo* in the yolk sac and formed more than evident cluster (red circle). Scale bar = 500  $\mu$ m. Combined treatment of quinacrine and quizartinib effectively ameliorated the myeloid expansion phenotype in *FLT3*-ITD-expressing zebrafish embryos (S-iii). (T–V) KEGG (T) and GSEA (U) analysis of PLA2G4A-correlated genes were performed by SangerBox program using TCGA-LAML database. Pantothenate and CoA biosynthesis was highlighted based on its significant normalized enrichment score (NES) (V). (W) Proposed working model showing the potential impacts of *FLT3*-ITD/ERK/PLA2G4A-mediated pantothenate and CoA biosynthesis in human AML. (X, Y) The correlation between PLA2G4A expression and infiltrations of immune cells was analyzed in TCGA-LAML by ESTIMATE (X) or CIBERSOR (Y) algorithms using SangerBox program, respectively. (Z) Proposed model of PLA2G4A-mediated leukemogenesis and immunosuppression in human *FLT3*-ITD<sup>+</sup> AML. Abbreviations: CoA: coenzyme A; COASY: coenzyme A synthase; Pan: pantothenate; PANK1: Pantothenate kinase 1; PPan: 4'-phosphopantothenate; PPanSH: 4'-phosphopantetheine; PPCS: phosphopantothoeylcysteine synthetase; SMVT: sodium-dependent multivitamin transporter; *VNN1*: Vanin1.

## Author contributions

B.L.H., A.Y.H.L. and W.J.L. conceived the project, designed the experiments and wrote the manuscript. W.J.L. and F.C. carried out the experiments with the assistance. L.S., X.M.Y. and J.Y. J.B.X. and A.Y.H.L. collected primary samples and analyzed clinical data. W.J.L, F.C., L.S. X.M.Y, J.Y., J.B.X, and B.L.H. analyzed and visualized the data. W.J.L, F.C., L.S. X.M.Y, J.Y., J.B.X, A.Y.H.L, and B.L.H. reviewed and edited the manuscript. B.L.H. directed and supervised the project. All authors discussed the results and commented on the manuscript.

## Conflict of interests

The authors declare no conflict of interests.

## Funding

This project was supported by grants from Theme-based Research Scheme of the Research Grants Council (Hong-kong) (No. T12-707/20-N, A.Y.H. Leung.), National Natural Science Foundation of China (No. 32000569, B.L. He) and GuangDong Basic and Applied Basic Research Foundation, China (No. 2019A1515110281, B.L. He).

## Acknowledgements

We thank the technical supports from Zebrafish Core Facility and Animal Units from The University of Hong Kong and The Fifth Affiliated Hospital of Sun Yat-sen University.

## Appendix A. Supplementary data

Supplementary data to this article can be found online at <https://doi.org/10.1016/j.gendis.2022.02.002>.

## References

1. Newell LF, Cook RJ. Advances in acute myeloid leukemia. *BMJ*. 2021;375:n2026.

2. He BL, Yang N, Man CH, et al. Follistatin is a novel therapeutic target and biomarker in FLT3/ITD acute myeloid leukemia. *EMBO Mol Med*. 2020;12(4):e10895.
3. Peng Z, Chang Y, Fan J, et al. Phospholipase A2 superfamily in cancer. *Cancer Lett*. 2021;497:165–177.
4. He BL, Shi X, Man CH, et al. Functions of flt3 in zebrafish hematopoiesis and its relevance to human acute myeloid leukemia. *Blood*. 2014;123(16):2518–2529.
5. Zhan Y, Zheng L, Liu J, et al. PLA2G4A promotes right-sided colorectal cancer progression by inducing CD39<sup>+</sup>γδ Treg polarization. *JCI Insight*. 2021;6(16):e148028.

Wen-Jing Lai<sup>a</sup>, Fan Chen<sup>a</sup>, Lingling Shu<sup>b</sup>, Xin-Ming Yang<sup>a</sup>, Jimin Yuan<sup>c</sup>, Jing-Bo Xu<sup>d</sup>, Anskar Yu-Hung Leung<sup>e,\*\*</sup>, Bai-Liang He<sup>a,\*</sup>

<sup>a</sup>Guangdong Provincial Key Laboratory of Biomedical Imaging, Guangdong Provincial Engineering Research Center of Molecular Imaging, The Fifth Affiliated Hospital, Sun Yat-sen University, Zhuhai, Guangdong 519000, China

<sup>b</sup>Department of Hematologic Oncology, State Key Laboratory of Oncology in South China, Collaborative Innovation Center for Cancer Medicine, Sun Yat-sen University Cancer Center, Guangzhou, Guangdong 510060, China

<sup>c</sup>Department of Geriatric Medicine, Shenzhen People's Hospital (The Second Clinical Medical College, Jinan University, The First Affiliated Hospital, Southern University of Science and Technology), Shenzhen, Guangdong 518020, China

<sup>d</sup>Department of Hematology, The Fifth Affiliated Hospital, Sun Yat-sen University, Zhuhai, Guangdong 519000, China

<sup>e</sup>Division of Haematology, Department of Medicine, Li Ka Shing Faculty of Medicine, The University of Hong Kong, Pokfulam, Hong Kong 999077, China

\*Corresponding author.

\*\*Corresponding author.

E-mail addresses: [ayhleung@hku.hk](mailto:ayhleung@hku.hk) (A.Y.-H. Leung), [hebliang@mail.sysu.edu.cn](mailto:hebliang@mail.sysu.edu.cn) (B.-L. He)

2 December 2021

Available online 12 March 2022